

## Laboratory study of the PDX/PLT laser blowoff trace element injectors

D. Manos, D. Ruzic, R. Moore, and S. Cohen

Citation: *J. Vac. Sci. Technol.* **20**, 1230 (1982); doi: 10.1116/1.571549

View online: <http://dx.doi.org/10.1116/1.571549>

View Table of Contents: <http://avspublications.org/jvst/cresource/1/JVSTAL/v20/i4>

Published by the AVS: Science & Technology of Materials, Interfaces, and Processing

---

### Related Articles

Analysis of unstable species in cyclo-C<sub>4</sub>F<sub>8</sub> plasma by ion attachment mass spectrometry

*J. Vac. Sci. Technol. A* **24**, 385 (2006)

Threshold ionization mass spectrometry of reactive species in remote Ar/C<sub>2</sub>H<sub>2</sub> expanding thermal plasma

*J. Vac. Sci. Technol. A* **23**, 1400 (2005)

Measurement of absolute radical densities in a plasma using modulated-beam line-of-sight threshold ionization mass spectrometry

*J. Vac. Sci. Technol. A* **22**, 71 (2004)

Measurement of the plasma potential adjacent to the substrate in a midfrequency bipolar pulsed magnetron

*J. Vac. Sci. Technol. A* **21**, L28 (2003)

Ion energy distributions and the density of CH<sub>3</sub> radicals in a low pressure inductively coupled CH<sub>4</sub>/H<sub>2</sub> plasma used for nanocrystalline diamond deposition


*J. Vac. Sci. Technol. A* **21**, 1988 (2003)

---

### Additional information on *J. Vac. Sci. Technol.*

Journal Homepage: <http://avspublications.org/jvst/resource/1/jvstal>

## ADVERTISEMENT




### Aluminum Valves with Conflat® Flanges

Less Outgassing Than Stainless  
Mate to Stainless Steel Conflats  
Sizes From 2.75 to 14 inch O.D.  
Leak Rate Less Than 10<sup>-10</sup> SCC/S

Visit us  
at Booth # 300  
in Tampa

Prices & Specifications  
[vacuumresearch.com](http://vacuumresearch.com)



# Laboratory study of the PDX/PLT laser blow-off trace element injectors<sup>a)</sup>

D. Manos, D. Ruzic, R. Moore, and S. Cohen

*Plasma Physics Laboratory, Princeton University, Princeton, New Jersey 08544*

(Received 21 September 1981; accepted 12 October 1981)

A laboratory study of the beams produced by laser blow-off trace element injectors used on the PDX and PLT tokamaks has been conducted. Eight target materials were studied, in the form of thin films on glass substrates: Al, Si, Sc, Cr, Fe, Ni, Cu, and Mo. Beam detectors included a quadrupole mass spectrometer, gridded retarding field analyzer, and beam collector plates. The collector plates were later analyzed by optical and electron microscopy and Auger spectroscopy. The results show that the injection produces the following species, in the usual order of decreasing velocity: free electrons, plasma, free ions, highly excited neutral atoms, unexcited neutral atoms, and metal clusters having diameters ranging up to several microns. The percentages of the various species, as well as their distributions of velocities, were found to be strong functions of the metal used, the film thickness, and the laser power density. Monoatomic species are generally contained within a half angle of  $\sim 12^\circ$ , while clusters are within  $\sim 5^\circ$ . Models of the production mechanism and implications for the use of the device as a tokamak diagnostic are discussed.

PACS numbers: 52.70.Nc, 52.40.Mj, 52.25.Lp, 52.55.Gb

## I. INTRODUCTION

Laser blow-off trace element injection has been frequently employed as a tokamak diagnostic.<sup>1</sup> Since its first application,<sup>2</sup> the injector parameter range has greatly changed to accommodate the requirements of newer tokamaks. This paper describes laboratory studies extending the previously reported<sup>2,3</sup> range of target materials, material thickness, and laser operating conditions.

## II. APPARATUS

The apparatus used in these studies is a modified version of that shown in Fig. 2 of Ref. 4. The 1.4 cm diam beam of a Q-switched ruby laser [ $1.2 \pm 0.3$  Joules, 20 ns FWHM] is focussed to 1–10 mm diam spots on 0.5–10  $\mu$  films deposited on glass slides. The ablated material beam transits a drift tube ( $p < 1.5 \times 10^{-6}$  Pa) to impinge on various detectors. The detectors include a quadrupole mass filter (QMF) system with an axial electron bombardment ionizer and off-axis Channeltron multiplier located 1.65 m from the laser target, and a retractable retarding field analyzer (RFA) located 1.0 m from the laser target. At distances from 1 to 100 cm from the laser target, 4.5 cm<sup>2</sup> metal-coated glass plates can be positioned to collect the beam. These plates can be examined by optical and electron microscopy and Auger spectroscopy to provide information regarding the size, number, and angular distribution of clusters present in the beam.

## III. RESULTS

Analysis of our QMF and RFA signals shows evidence for free electrons, ions, plasma, and neutral atoms. Both devices display fast pulses, or "spikes," which Marmor *et al.*,<sup>2</sup> attributed to clusters. We employed strong electric and magnetic deflecting fields to remove the charged particles from the beams. The tokamak magnetic fields are expected to do likewise.

### A. Unexcited neutral atoms

Except for Mo, the neutral atom fraction of the beam comprises excited and unexcited atoms, the latter appearing as an ionizer dependent signal in the QMF. For Mo no unexcited neutral signal appeared.

Mass selected time-of-flight signals were recorded for a variety of thicknesses of several materials at different laser energy densities (fluences). The detailed distributions are presented elsewhere.<sup>4</sup> The average translational energy of the resulting distributions is plotted as a function of fluence in Fig. 1. Figure 1(b) shows the effect of changing thickness for scandium. As the target thickness increases it becomes progressively more difficult to measure the unexcited neutral atom signal because of an increase in the frequency and magnitude of spikes. As the fluence increases, these spikes shift to earlier arrival times, obscuring the neutral peak. The magnitude of the neutral signal increases nearly quadratically with target thickness up to 5  $\mu$  and then decreases linearly to  $\frac{1}{10}$  this peak value at 10  $\mu$ .

The angular distribution of the neutral atom component is shown for 1  $\mu$  targets in Fig. 2. For these thin films, half of the neutral atom beam is within  $\theta = 10^\circ$ – $15^\circ$ , where  $\theta$  is the half-angle measured from the surface normal. These data are for laser fluences  $\sim 50$  J/cm<sup>2</sup> where the frequency of spikes is relatively low. We note that the frequency of spikes decreased a factor of 10 as  $\theta$  increased from normal incidence to  $\pm 5^\circ$ .

### B. Excited neutral atoms

The existence of a smoothly varying QMS signal independent of ionizer current or mass selectivity suggests an atomic beam component capable of producing ions on impact with cold surfaces. Candidates are metastable or Rydberg<sup>5</sup> states, although evidence for cold surface ionization predominantly by conversion of translational energy exists.<sup>6</sup>

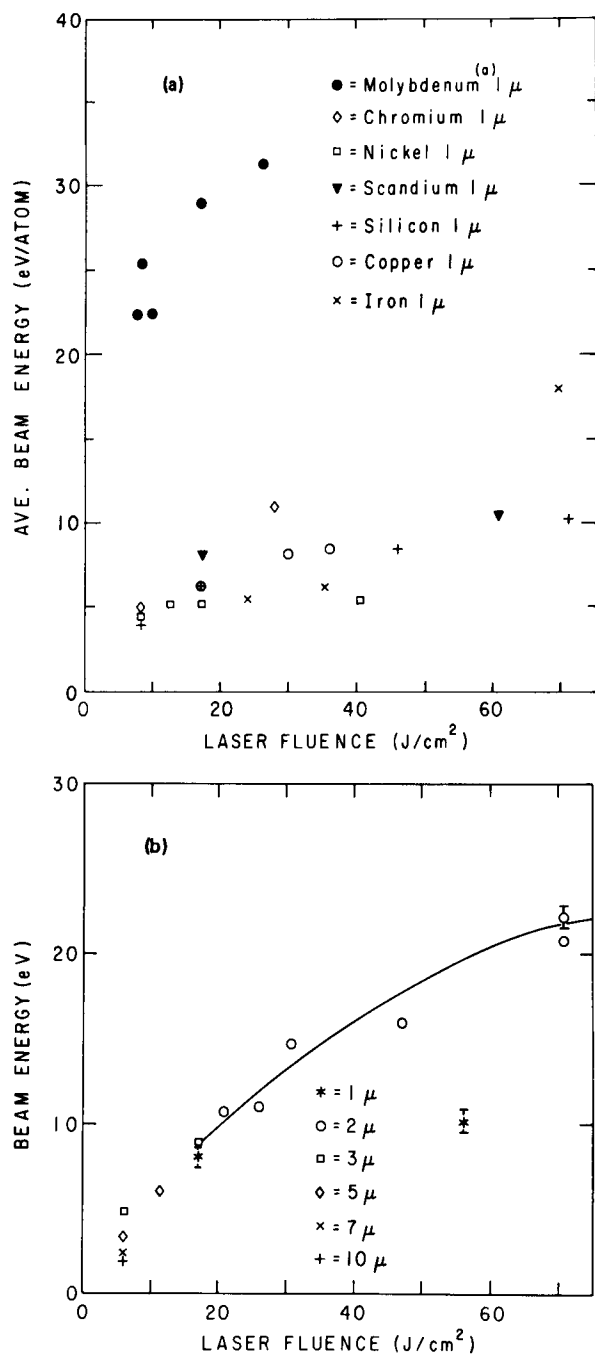


FIG. 1. (a) Average translational energy for neutral atoms formed from 1  $\mu$  metal films as a function of laser fluence. Note that Mo forms only excited state neutrals; for all other metals the unexcited neutral energy is plotted. The excited states for the other metals would lie less than 50% higher than the unexcited states on this plot. (b) Average beam energy vs laser fluence for various thicknesses of Sc films. Formation of high velocity clusters precludes measurement of neutrals at high fluence for targets thicker than 3  $\mu$ .

For Rydberg atoms to account for excited atom signals as late as 250–300  $\mu$ s after the laser pulse would require principle quantum numbers of  $n \gtrsim 60$  (for  $l = 0$ ).<sup>5</sup> Electric fields up to 20 kV/cm, which should readily ionize all states having  $n \gtrsim 7$ , had no noticeable effect on this QMS signal. Varying background gas pressure from  $1.5 \times 10^{-6}$  Pa to  $3 \times 10^{-3}$  Pa caused an increase in excited atom signal,  $I \propto P^{1/2}$ , also suggesting that high Rydberg states are not the carrier of this

signal. This pressure dependence is discussed further in Ref. 4.

### C. Clusters

Spikes were observed in the QMF and RFA signals for all materials studied except 1  $\mu$  thick Si and 0.5  $\mu$  thick Al; 1  $\mu$  Cr also showed little spiking at any fluence. One observes that the frequency and magnitude of the spikes increase as target thickness increases. For targets thicker than 2  $\mu$ , as the laser fluence increases, the distribution of spikes shifts to earlier arrival times, the number of spikes decreases, and their magnitude increases. For targets thinner than 2  $\mu$ , the same temporal shift is observed as fluence increases, but the number of spikes decreases faster and the magnitude is unchanged until the spikes become almost entirely absent above 100 J/cm².

Examination of collector plates placed downstream in the beam confirmed the presence of microscopic projectiles moving at velocities sufficiently high to form craters in the surfaces. Targets of 1  $\mu$  Si, 0.5  $\mu$  Al, and 1  $\mu$  Cr produced less

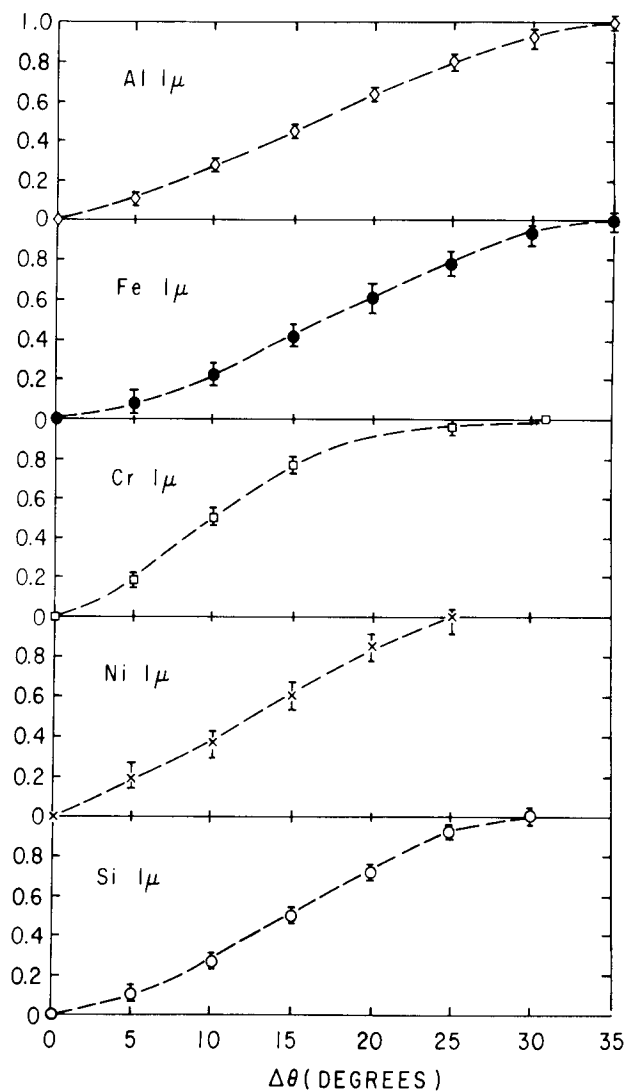


FIG. 2. Angle integrated angular distributions of unexcited neutral atoms for 1  $\mu$  films. Plots are based on QMF signals recorded as the laser target is rotated about an axis perpendicular to the laser beam.

than 10 times fewer craters than Fe, Cu, or Sc targets of similar thicknesses. Examples of optical and electron micrographs for Sc targets are shown in Fig. 3. A comparison of Figs. 3(a) and (b) shows the difference between the portions of the plate exposed to and shielded from the beam. The crater-like nature of the surface features is shown in (c) and (d). SEM's with magnification up to  $\times 9000$  showed that for all materials and thicknesses studied no craters smaller than  $\approx \frac{1}{4} \mu$  were present.

Cluster number and size distributions, derived from counts of the micrographs, correlate well with the QMF (RFA) spike behavior. From the material properties and QMF determined cluster velocity, the crater radius is estimated to be one to two times the cluster radius.<sup>7</sup> From these distributions, total percentages of the beam in the cluster component are derived.

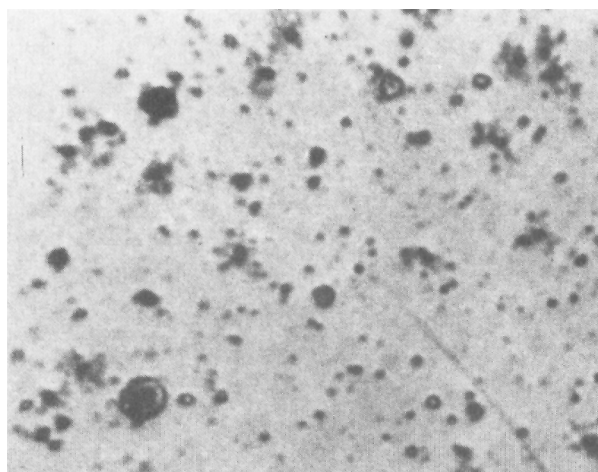
The following percentages were found under the assumption of equal crater and cluster radii. Clusters are more common for thicker targets and for lower laser fluence.

5 J/cm <sup>2</sup> :	Al, $1 \mu \approx 7\%$ ; Si, $1 \mu \approx 0\%$ ; Sc, $1 \mu = 9\%-14\%$ ; Cr, $1 \mu < 1\%$ ; Fe, $1 \mu = 40\%-60\%$ ; Ni, $1 \mu = 30\%-50\%$ ; Sc, $3 \mu \approx 50\%$ ; Sc, $5 \mu \approx 80\%$ ; Sc, $7 \mu \approx 100\%$ .
12 J/cm <sup>2</sup> :	Sc, $1 \mu \approx 11\%$ ; Sc, $3 \mu \approx 8\%-15\%$ ; Sc, $7 \mu \approx 100\%$ .
25 J/cm <sup>2</sup> :	Sc, $1 \mu = 0\%-1\%$ ; Sc, $2 \mu = 5\%-15\%$ ; Sc, $3 \mu = 50\%-60\%$ ; Sc, $5 \mu = 65\%-100\%$ ; Sc, $7 \mu = 75\%-100\%$ .
140 J/cm <sup>2</sup> :	Sc, $1 \mu \approx 0\%$ ; Sc, $7 \mu \approx 70\%$ .

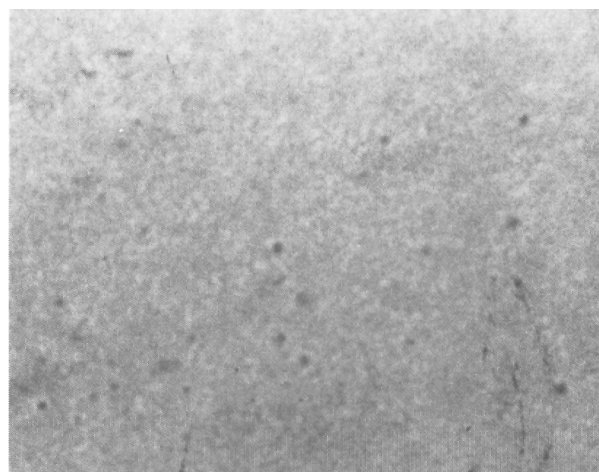
Point and line Auger spectroscopy confirms that for Sc targets thicker than  $3 \mu$ , more than 99% of the collected material can be present in the cratered regions.

Examination of the collector plates employed at varying

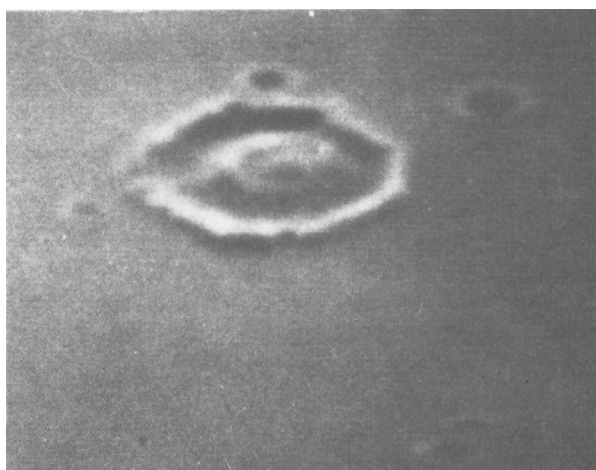
distances from the laser targets allows an estimate of the angular distribution of clusters. For targets less than  $3 \mu$  thick, clusters are contained with a FWHM of  $5^\circ$ – $10^\circ$ . For  $3$ – $10 \mu$  Sc the FWHM does not exceed  $3^\circ$ – $5^\circ$ .



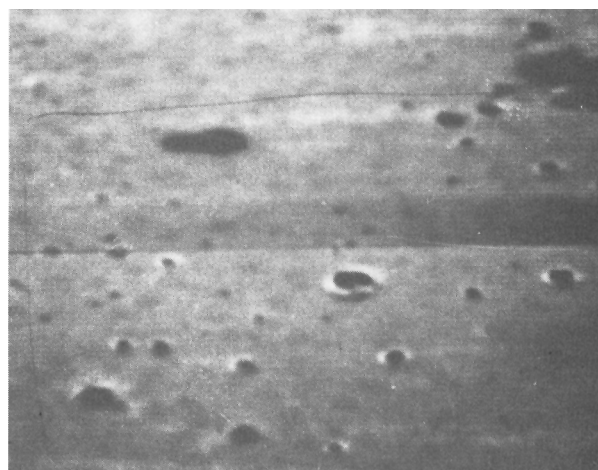
(a)



(b)



(c)



(d)

FIG. 3. (a) Optical micrograph of collector plate exposed to beam produced by  $3 \mu$  Sc. The scale is  $1 \text{ cm} = 14 \mu$ . (b) Same as (a), showing region of collector protected by 2 mm Al foil during beam exposure. (c) Scanning electron micrograph of exposed region of target plot, the scale is  $1 \text{ cm} = 1.4 \mu$ . (d) Scanning electron micrograph of exposed region of target plate. The scale is  $1 \text{ cm} = 6.9 \mu$ .

#### IV. DISCUSSION

Although the details of beam production are very complicated, this experiment shares many features of recent planar ablative-pusher, laser-fusion experiments.<sup>8</sup> Based on these experiments the following tentative mechanistic sequence is proposed.

At the onset of the laser pulse the irradiated disk breaks away from the surrounding metal on a time scale comparable to the passage of the resulting shock to the forward surface ( $<1$  ns). The disk is strongly accelerated by the nearly isothermal plasma for the duration of the pulse,  $\tau \simeq 20$  ns, and to a lesser extent by the expansion of the plasma for a short time thereafter. In the case on thin targets, thickness  $\leq (k\tau/C_p \rho)^{1/2} \simeq 1.5 \mu$ , this acceleration period is long enough to allow thermal conduction to heat the entire film to  $\geq 2600^\circ\text{C}$ . At this temperature, evaporation is sufficient to cause complete atomization.

For thicker targets, several mechanisms may be working to fragment the disk during the acceleration. An interaction of acoustic instabilities, introduced by the presence of the glass slide, with the shock may cause the disk to disintegrate as the shock unloads at the forward surface. A likely cause is hot spots in the laser beam leading to an inhomogeneous pressure at the rear surface. Hot spots several microns in size have been reported for laser systems identical to ours.<sup>9</sup> Another possible cause is Rayleigh–Taylor instability as the rarified plasma accelerates the dense disk. A calculation of the mode of maximal Rayleigh–Taylor instability for Fe yields a wavenumber of  $k^* \simeq 1.3 \times 10^5$  corresponding to a predicted instability scale length of  $\approx \frac{1}{4} \mu$ . This assumes: (a) that the surface tension of the dense phase equals that of the bulk liquid at its melting point, (b) that the plasma is, on the average, half as dense as the dense phase, and (c) that the acceleration is uniform and yields the average laboratory velocity of the clusters during the laser pulse. For the other materials studied the scale length is also  $\approx \frac{1}{4} \mu$ . The agreement of this scale length and the smallest crater size seen under any circumstances may be a coincidence since there are physical mechanisms,<sup>10</sup> such as “fire polishing” and laser oscillation stabilization, that predict damping of Rayleigh–Taylor instabilities. Craters having diameters significantly larger than the laser target thickness are assumed to be formed by the impact of disks, rather than spheres. Evidence to support this is found in SEM photographs which show disk and needle shaped objects embedded edge-on into the collectors. Such fragments achieve sizes up to almost  $100 \mu$  for the case of  $7 \mu \text{ Sc}$  at  $10 \text{ J/cm}^2$ .

#### V. APPLICATION TO TOKAMAKS

We have demonstrated that there are two distinct operational regimes of the injector: cluster and monoatomic beams. These are individually accessible by controlling four parameters; material, material thickness, angle, and laser fluence. In addition, the energy distribution within each regime can be varied an order of magnitude. This latter property allows study of scrape-off penetration.

Impurity transport studies have relied on seeding the edge of the plasma with individual atoms. However microscopic ( $\frac{1}{4}$ – $100 \mu$ ) clusters moving at  $5 \times 10^5 \text{ cm/s}$  will penetrate up to  $25 \text{ cm}$  into the tokamak plasma. This offers the possibility for new types of impurity studies where edge loss is not as important a process in the early time evolution of the spectral lines.

The formation of large clusters may also allow injection of other entrapped nonmetallic elements. One example is tritiated metal films for which studies are now in progress.

#### ACKNOWLEDGMENTS

The authors would like to thank J. Boris and T. Gallagher for helpful discussions regarding this work.

<sup>a</sup>Supported by the U. S. Department of Energy, Contract No. DE-AC02-76-CH03073 and the Fannie and John Hertz Foundation.

<sup>1</sup>See, for example, S. Suckewer, J. Cecchi, S. Cohen, R. Fonck, and E. Hinnov, *Phys. Lett.* **80A**, 259 (1980).

<sup>2</sup>E. S. Marmor, J. L. Cecchi, and S. A. Cohen, *Rev. Sci. Instrum.* **46**, 1149 (1975).

<sup>3</sup>J. F. Friichtenicht, *Rev. Sci. Instrum.* **45**, 51 (1974).

<sup>4</sup>D. M. Manos, D. Ruzic, R. Moore, and S. A. Cohen, PPPL Matt Rep. (in preparation).

<sup>5</sup>S. A. Edelstein and T. F. Gallagher, *Advances in Atomic and Molecular Physics*, (Academic, New York, 1978), Vol. 14, p. 365.

<sup>6</sup>R. P. Stein and F. C. Hurlbut, *Phys. Rev.* **123**, 790 (1961).

<sup>7</sup>N. R. Sorensen, NAVWEPS Rep. 8585; NOTS Technical Publication 3593, August 1964.

<sup>8</sup>J. Grun, NRL Memorandum Rep. 4491, May 8, 1981.

<sup>9</sup>J. F. Giuliani and W. T. Anderson, Jr., *Appl. Opt.* **20**, 2597 (1981).

<sup>10</sup>J. Boris, NRL Memorandum Rep. 3427 (1976).